Tumor-associated macrophages suppress estrogen receptor-β expression in triple-negative breast cancer through the PI3K/AKT pathway

QIULEI ZHANG[1,2*], DI GUO[3*], GAORAN XU[1,2], RONG XIE[1], YUQING DENG[1], PENG FU[1*] and JINNAN WAN[1*]

[1]Department of Thyroid and Breast Surgery, The Central Hospital of Wuhan, Tongji Medical College, Huazhong University of Science and Technology, Wuhan, Hubei 430014, P.R. China; [2]Key Laboratory for Molecular Diagnosis of Hubei, The Central Hospital of Wuhan, Tongji Medical College, Huazhong University of Science and Technology, Wuhan, Hubei 430014, P.R. China; [3]Department of Internal Medicine, Central China Normal University Hospital, Central China Normal University, Wuhan, Hubei 430079, P.R. China

Received June 11, 2025; Accepted November 3, 2025

DOI: 10.3892/etm.2026.13072

Abstract. Triple-negative breast cancer (TNBC) is a highly aggressive breast cancer subtype with limited therapeutic options. Estrogen receptor (ER)-β exerts anti-tumor effects. However, ERβ expression is frequently reduced in TNBC and the mechanisms underlying the downregulation of ERβ in TNBC remain poorly understood. In the present study, findings revealed that tumor-associated macrophages (TAMs), which are abundant in the tumor microenvironment, suppressed ERβ expression in TNBC cells. The relationship between TAMs and ERβ in TNBC was investigated through bioinformatics analysis, co-culture and orthotopic mouse models. ERβ expression levels were lower in the TNBC tumors compared with normal tissues. Mechanistically, TAM-induced activation of the PI3K/AKT pathway suppressed ERβ expression by reducing FOXO3a binding to the ESR2 promoter, whereas inhibition of PI3K/AKT restored ERβ expression. Notably, combined PI3K/AKT pathway inhibition with ERβ activation attenuated TNBC cell metastasis. Overall, findings indicated that TAMs promoted TNBC progression by downregulating ERβ expression through the PI3K/AKT/FOXO3a axis, highlighting the therapeutic potential of combining PI3K/AKT inhibitors with ERβ agonists in TNBC.

Correspondence to: Dr Peng Fu or Dr Jinnan Wan, Department of Thyroid and Breast Surgery, The Central Hospital of Wuhan, Tongji Medical College, Huazhong University of Science and Technology, 26 Shengli Street, Wuhan, Hubei 430014, P.R. China
E-mail: fupeng202303@163.com
E-mail: 13720303601@163.com

*Contributed equally

Key words: triple-negative breast cancer, ERβ, tumor-associated macrophages, PI3K/AKT pathway, mouse model

Introduction

Breast cancer is among the most prevalent malignancies in women worldwide (1). Triple-negative breast cancer (TNBC) is an aggressive breast cancer subtype characterized by the absence of estrogen receptors (ERs), progesterone receptors and human epidermal growth factor receptor-2 (HER-2). Therefore, it does not respond to typical endocrine and anti-HER-2 therapies. Consequently, TNBC is associated with higher recurrence and metastasis rates compared with other breast cancer subtypes. Current treatment strategies primarily rely on chemotherapy, however the outcomes remain suboptimal (2), necessitating the identification of novel therapeutic targets.

ERβ [also known as estrogen receptor 2 (ESR2)] is highly expressed in normal breast tissues, however expression is markedly decreased during breast carcinogenesis (3-6). ERβ is detected in all breast cancer subtypes, especially in TNBC, with ~30% of TNBC tumors expressing ERβ and elevated ERβ levels being associated with its favorable prognosis (7,8). Preclinical studies have demonstrated the tumor-suppressive role of ERβ (9-11), highlighting it as a promising therapeutic target for TNBC. However, the mechanisms driving this downregulation remain unclear.

Tumor-associated macrophages (TAMs) are key components of the breast cancer microenvironment. High TAM infiltration is associated with poor prognosis (12-14). TAMs regulate ERα expression in cancer cells (15,16). However, the specific association between TAMs and ERβ expression and the mechanisms by which TAMs regulate ERβ expression remains unknown. Therefore, in the present study, the association between TAMs and ERβ expression in TNBC cells was investigated and the molecular mechanisms underlying TAM-mediated ERβ suppression was explored.

Materials and methods

Mice and cell lines. Female BALB/c mice (6-8 weeks old; 20-25 g) were housed in a pathogen-free facility at the Experimental

Animal Center of Tongji Medical College, Huazhong University of Science and Technology (Wuhan, China). The animals were maintained at a constant temperature of 22±2˚C and a relative humidity of 50±10% under a 12-h light/dark cycle, with free access to food and water. All procedures were approved by the Institutional Animal Care and Use Committee of Huazhong University of Science and Technology. Following tumor cell implantation, mice (n=12) were monitored every 2 days for body weight, behavior, tumor size and vital signs, with food, water and bedding refreshed as needed. Humane endpoints included >20% body weight loss, dyspnea, tumor ulceration/necrosis or inability to access food and water. Based on prior reports and preliminary studies, mice were sacrificed at week 5 to allow assessment of pulmonary metastases while minimizing mortality. Sacrifice was performed with intraperitoneal sodium pentobarbital (50 mg/kg) followed by cervical dislocation and mortality was verified by absence of heartbeat, respiration and corneal reflexes. The murine 4T1 cell line was purchased from the Cell Bank of the Chinese Academy of Sciences (Shanghai, China) and incubated in humidified conditions at 37˚C. Bone marrow-derived macrophages with M2 polarization and conditioned medium (CM) from M2 macrophages were obtained as previously described (17).

Data acquisition. Expression profiles and related clinical data of patients with TNBC were obtained from The Cancer Genome Atlas (TCGA) datasets (https://portal.gdc.cancer.gov/). Single-cell RNA sequencing datasets were downloaded from the Gene Expression Omnibus database [GEO; https://www.ncbi.nlm.nih.gov/geo/; GSE202624 (18)]. UCALAN (http://ualcan.path.uab.edu/) was used to compare the ESR2 mRNA levels among breast cancer gene (BRCA) subtypes and Human Protein Atlas (HPA; https://www.proteinatlas.org/) datasets were used to compare the ERβ protein levels between breast cancer and normal tissues. AnimalTFDB (version 4.0; https://guolab.wchscu.cn/AnimalTFDB4) was used to predict transcription factor (TF) binding sites.

Bioinformatics analysis. Bioinformatics analyses of the data of patients with TNBC obtained from TCGA and single-cell RNA sequencing datasets (GEO: GSE202624) were performed using R (version 4.0.2; http://www.R-project.org). Kyoto Encyclopedia of Genes and Genomes (KEGG) pathway analysis and gene set enrichment analysis (GSEA) of differentially expressed genes were performed using the 'ClusterProfiler' R package (version 3.8; https://bioconductor.org/packages/clusterProfiler/). Survival statistics were plotted using the K-M Plotter database (https://kmplot.com/). Immune infiltration and mRNA expression data from Gene Set Cancer Analysis (GSCA; https://guolab.wchscu.cn/GSCA) were used to investigate the association between mRNA expression and immune cell infiltration through Spearman's rank correlation analysis. Additionally, the Tumor Immune Estimation Resource 2.0 database (TIMER2.0; http://timer.cistrome.org/) was used to explore the association between macrophage scavenger receptor 1 (MSR1) and a number of epithelial-mesenchymal transition (EMT) markers in TNBC.

Reverse transcription quantitative PCR (RT-qPCR). RNAiso Plus (Takara Bio, Inc.) was used to extract the total RNA of 4T1 cells, which was reverse transcribed into cDNA using the ReverTra Ace™ qPCR RT Kit (Toyobo Co., Ltd.) according to the manufacturer's instructions. qPCR analyses with SYBR® Green Real Time PCR Master Mix (Toyobo Co., Ltd.) and specific primers were performed to measure the target gene mRNA transcript levels relative to the β-actin levels. The thermocycling conditions were as follows: Initial denaturation at 95˚C for 1 min; 40 cycles of 95˚C for 5 sec (denaturation), 60˚C for 15 sec (annealing) and 72˚C for 45 sec (extension), with fluorescence data collection. A melting-curve analysis was performed at the end of each run to confirm the specificity of amplification. All reactions were carried out according to the manufacturers' protocols. Data were normalized to the β-actin levels and analyzed through the $2^{-\Delta\Delta Cq}$ method (19). All primer sequences are listed in the Table SI.

Mouse model of breast cancer and macrophage depletion. 4T1 cell lines ($1x10^6$) were injected into the mammary fat pads of BALB/c mice. Clodronate liposomes obtained from Vrije Universiteit (Amsterdam) were used to deplete the macrophages, as previously described (17). LY294002 (MedChemExpress), a selective PI3K inhibitor, was dissolved at 5 mg/ml in 10% DMSO and intraperitoneally injected at 50 mg/kg (200 μl/injection), twice weekly for five weeks (20,21). ERB041 (Tocris Bioscience), an ERβ-selective agonist, was dissolved at 2 mg/ml in 10% DMSO and administered subcutaneously at 5 mg/kg (50 μl/injection) once daily for five weeks, as previously described (22). For vehicle controls, mice received injections of 10% DMSO in 90% corn oil. Tumor volume was calculated as follows: Volume=(length x width x width)/2.

Immunofluorescence assay and immunohistochemistry. Mouse breast tumor paraffin-embedded sections (4 μm) were stained with specific primary antibodies overnight at 4˚C. The bound antibodies were detected using CoraLite488-goat anti-rabbit IgG (1:400; cat. no. SA00013-2; Proteintech Group, Inc.) and Coralite594-goat anti-rabbit IgG (1:400; cat. no. SA00013-4; Proteintech Group, Inc.) at room temperature for 30 min. DAPI (Wuhan Servicebio Technology Co., Ltd.) was used to stain the nuclei at room temperature for 10 min in the dark. Finally, the cells were observed under a laser confocal microscope (Olympus Corporation). All antibodies used in the present study are listed in the Table SII.

TNBC tissues from two female patients (age, 45 and 63 years) were collected at The Central Hospital of Wuhan, Tongji Medical College, Huazhong University of Science and Technology between January 2022 and December 2023. The present study was approved by the Ethics Committee of The Central Hospital of Wuhan (China; approval no. WHZXKYL2022-033). Immunohistochemistry staining was performed by Wuhan Servicebio Technology Co., Ltd., on formalin-fixed, paraffin-embedded tissue sections. The procedures followed standard immunohistochemistry protocols, including deparaffinization, antigen retrieval, blocking, incubation with primary and secondary antibodies, and chromogenic detection. Slides were counterstained, dehydrated and mounted according to routine laboratory practices. All steps were carried out following the company's standard operating procedures.

Flow cytometry. 4T1 cells were cultured with M2 macrophages at 37˚C in a humidified atmosphere containing 5% CO_2 in the same dish for 24 h, washed with cold PBS and stained with anti-F4/80-BV421 (BD Pharmingen; BD Biosciences) and BV421 rat IgG isotype antibody (BioLegend, Inc.) for 30 min at 4˚C. Subsequently, the cells were fixed, made permeable (Fixation/Permeabilization Kit; cat. no. 554714; BD Pharmingen; BD Biosciences) according to the manufacturer's instructions, and intracellularly stained with anti-ERβ-phycoerythrin antibodies (Novus Biologicals) for 60 min at 4˚C. Flow cytometry (BD FACSAria™ II) was used to characterize the cells and FlowJo™ v10 software (BD Biosciences) was used for data analysis. Cells were first gated based on forward scatter (FSC) and side scatter (SSC) to select the live single-cell population, excluding debris and aggregates. Macrophages were gated for $F4/80^+$ and mean fluorescence intensity of ERβ in 4T1 cells ($F4/80^-$) was analyzed. All antibodies used in the present study are listed in Table SII.

Transwell assay and wound healing assay. After digestion with trypsin for 3 min at 37˚C, 4T1 cells were resuspended in a serum-free medium. Then, 200 μl cell suspension with $2x10^4$ cells was added to the upper chamber and 500 μl culture medium containing 10% fetal bovine serum (Wuhan Servicebio Technology Co., Ltd.) was added to the lower chamber of the Transwell system (Corning, Inc.) at 37˚C. After 24 h, the migrated cells were fixed with 4% paraformaldehyde and stained with crystal violet for 15 min at room temperature, images were acquired using an inverted light microscope (IX81; Olympus Corporation) and cells were counted using ImageJ software (version 1.8.0; National Institute of Health). Briefly, images were converted to 8-bit grayscale, the background was subtracted using the 'Subtract Background' function and cells were distinguished from the background by applying a threshold. The 'Analyze Particles' function was used to count cells, with size and circularity parameters adjusted to exclude debris. For each well, three random fields were analyzed, and the mean cell number was calculated. A total of $1x10^5$ cells were seeded in a six-well plate and cultured until they reached 90% confluence. A scratch was then created using a 20 μl pipette tip, then washed three times with PBS. Images were captured at 0 and 24 h to evaluate cell migration.

Chromatin immunoprecipitation (ChIP) assay. A total of $1x10^7$ 4T1 cells were used for each experimental condition. Briefly, 4T1 cells were fixed with 1% formaldehyde for 10 min at room temperature, and cross-linked protein-DNA complexes were extracted using the Magna ChIP® A/G Chromatin Immunoprecipitation Kit (cat. no. 17-10085; MilliporeSigma) according to the manufacturer's instructions. Immunoprecipitation was performed by overnight incubation at 4˚C with a primary antibody against FOXO3a or rabbit IgG under gentle rotation (Table SII), followed by incubation with magnetic beads at 4˚C for 2 h. DNA was purified from the complexes and analyzed through qPCR using primers targeting the FOXO3a binding site within the mouse ESR2 promoter (forward: 5'-GTGGGATAAGGGATTGTGAA-3'; reverse: 5'-AACGCAGGAGCAGAAGATAG-3'). ChIP signal enrichment was quantified by RT-qPCR and expressed as the signal-to-input ratio (fold enrichment=$100x2^{\Delta Cq}$). Amplified products were resolved by 1.5% agarose gel electrophoresis in 1X TAE buffer, stained with ethidium bromide and detected under a UV transilluminator.

Statistical analysis. Statistical analyses were conducted using the GraphPad Prism (version 8.0; GraphPad; Dotmatics) software. Differences between two groups were evaluated using an unpaired Student's t-test, while comparisons among three or more groups were analyzed using one-way ANOVA followed by Tukey's post-hoc test. Results are represented as the mean ± standard deviation. $P<0.05$ was considered to indicate a statistically significant difference. $^*P<0.05$, $^{**}P<0.01$ and $^{***}P<0.001$.

Results

Clinical value and expression of ERβ in TNBC. Survival analysis using GSCA data revealed that high ESR2 levels in patients with breast cancer were associated with improved progression-free survival (Fig. 1A) and overall survival (Fig. 1B). ESR2 levels were also found to differ among breast cancer subtypes (Fig. 1C), with TNBC showing the highest ESR2 levels (23). Further validation using the Cancer Cell Line Encyclopedia (24) demonstrated that TNBC cell lines expressed high ESR2 levels ($P<0.05$; Fig. 1D). Transwell assay results revealed that the pharmacological activation of ERβ effectively suppressed 4T1 cell migration ($P=0.003$; Fig. 1E), suggesting ERβ as a potential therapeutic target for TNBC. Furthermore, ESR2 expression levels were compared between normal and tumor tissues using TCGA data. Findings demonstrated that ESR2 levels were significantly downregulated in TNBC ($P<0.001$; Fig. 1F). Analysis of the HPA data (25) revealed that protein ERβ levels were lower in BRCA tissues compared with normal tissues (Fig. 1G). Results consistently showed lower ERβ levels in cancerous tissues compared with adjacent non-malignant tissues (Fig. 1H). Collectively, TNBC showed higher ERβ expression compared with other breast cancer subtypes, indicating its therapeutic potential. However, the levels remained markedly lower compared with those in normal breast tissues. The underlying mechanisms of ERβ downregulation remain to be elucidated and warrant further investigation.

TAMs enhance tumor metastasis in TNBC. TAM infiltration is a key feature of the breast cancer microenvironment and is associated with a poor prognosis. To assess the roles of TAMs in breast cancer, the expression levels of TAM marker MSR1 were examined using TCGA data. MSR1 levels were notably upregulated in the breast cancer tissues, including TNBC, compared with those in the adjacent normal tissues (Fig. 2A). Survival analysis revealed that high MSR1 expression was associated with poor overall survival in TNBC (log_{rank} $P=0.015$; Fig. 2B). Additionally, analysis of TIMER2.0 data (26) revealed positive correlations between EMT-related genes [such as matrix metalloproteinase (MMP)-9 and Twist2] and MSR1 levels in TNBC (Fig. 2C). GSEA was performed on single-cell RNA sequencing data from TAM-enriched and TAM-depleted mouse breast tumors (GEO: GSE202624), obtained from Seok *et al* (18). Findings revealed that EMT-associated genes in breast cancer were downregulated in the TAM-depleted group (Fig. 2D and E).

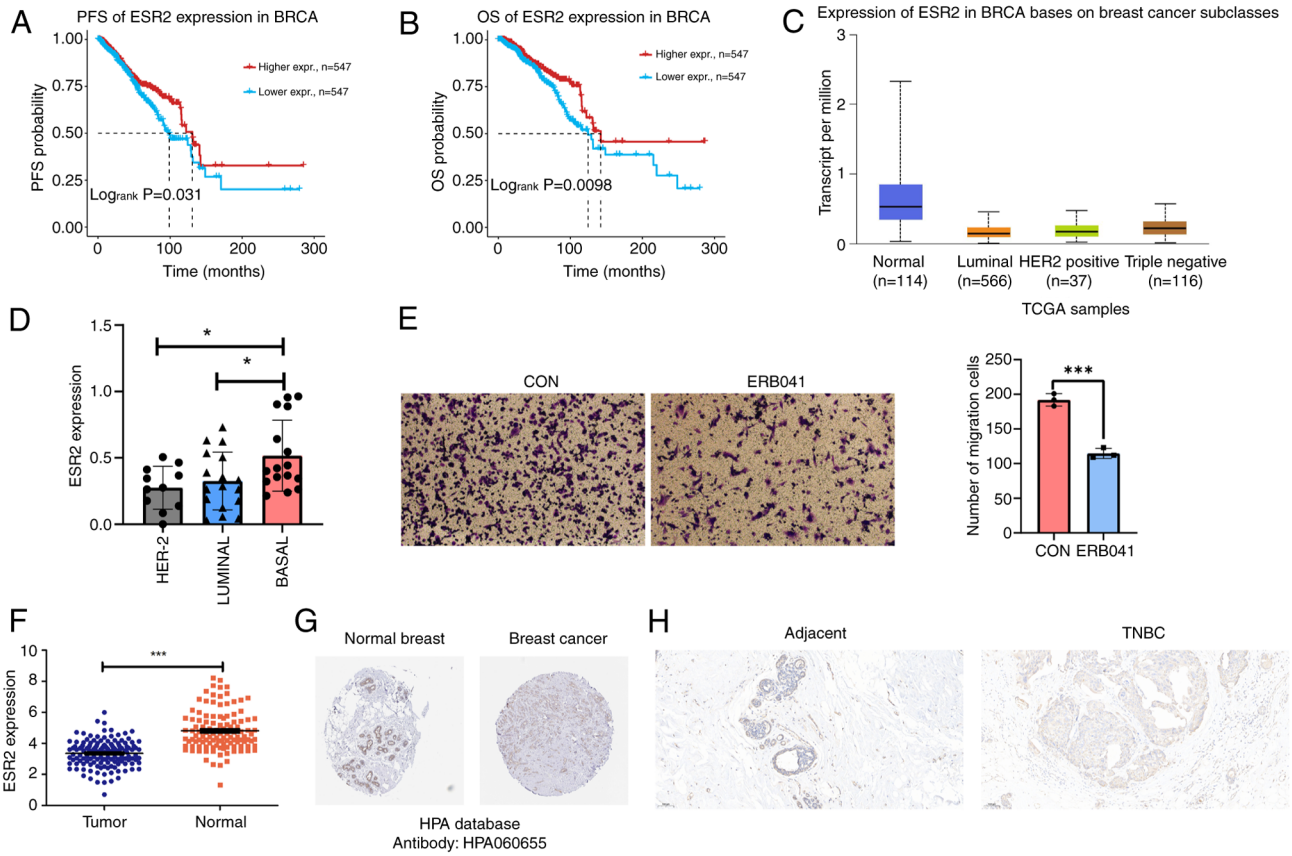

Figure 1. Clinical value and expression of ERβ (also known as ESR2) in TNBC. (A) PFS analysis of ESR2 levels in BRCA. (B) OS analysis of ESR2 levels in BRCA. (C) ESR2 mRNA levels in different BRCA subtypes. (D) ESR2 mRNA levels in different breast cancer subtype cell lines. (E) Migratory capacity of 4T1 cells treated with vehicle (ethanol) or ERβ agonist, ERB041 (100 nM), was assessed through Transwell assays. (F) Scatter plot showing the differentially expressed ESR2 between TNBC tumor and normal tissues. (G) Immunohistochemical staining from the Human Protein Atlas database revealed ERβ protein expression in both normal breast and BRCA tissues. (H) Immunohistochemistry was used to evaluate the ERβ expression levels in paracancerous and breast cancer tissues. Scale bar, 100 μm. Magnification, x100. *P<0.05 and ***P<0.001. Erβ, estrogen receptor-β; TNBC, triple negative breast cancer; PFS, progression-free survival; OS, overall survival; BRCA; breast cancer; HER-2, human epidermal growth factor receptor-2; CON, control; ns, not significant; TCGA, The Cancer Genome Atlas.

These findings suggested that TAMs notably enhance TNBC metastasis.

TAMs suppress ERβ expression in TNBC. Based on the aforementioned results, the correlation between ESR2 levels and TAMs in TNBC was explored. Correlation analysis using TCGA data revealed that TAM infiltration was negatively correlated with ERβ expression in BRCA (Fig. 3A and B). In breast cancer, TAMs mainly exhibit the M2 phenotype (17). To mimic the TNBC tumor microenvironment, M2-polarized macrophages and 4T1 cells were added to the upper and lower chambers of the Transwell system, respectively. ESR2 mRNA levels in 4T1 cells were markedly reduced in the M2 co-culture group (P<0.05; Fig. 3C). To further assess whether TAMs suppress ERβ expression, flow cytometry was used to analyze ERβ level after treatment with varying proportions of M2 macrophages. Notably, co-culture with M2 macrophages markedly reduced ERβ expression, as evidenced by the decreasing mean fluorescence intensity of ERβ in 4T1 cells with increasing macrophage proportions (P<0.001; Fig. 3D). Cellular immunofluorescence staining revealed that TAM-CM notably suppressed ERβ expression (Fig. 3E). Subsequently, clodronate liposomes were used to selectively deplete the macrophages in 4T1 mice model to validate findings *in vivo*. Immunofluorescence staining was used to analyze the tumor tissue sections. Compared with the control group, clodronate liposome-treated group showed markedly reduced $CD204^{+}$ TAM levels, associated with increased $ERβ^{+}$ tumor cell levels (Fig. 3F). These results collectively suggested TAMs inhibit ERβ expression in TNBC.

TAM-mediated ERβ suppression mechanisms. To elucidate TAM-mediated ERβ suppression mechanisms, TNBC samples from TCGA database were stratified into high and low TAM expression groups based on MSR1 levels. KEGG pathway analysis revealed significant enrichment of the 'PI3K-AKT signaling pathway' (Fig. 4A). Further validation using the GSCA database corroborated the differential activity of the PI3K/AKT pathway between the high and low MSR1 expression groups (Fig. 4B). TAMs are reported to activate tumor-intrinsic PI3K/AKT signaling across cancer types, promoting tumor invasion and therapy resistance in digestive tract tumors and ER^{+} breast cancer (27-29). The role of TAMs in modulating the PI3K/AKT pathway was further investigated using a 4T1 mouse model. Immunohistochemical analysis of tumor tissues revealed that clodronate liposome-mediated

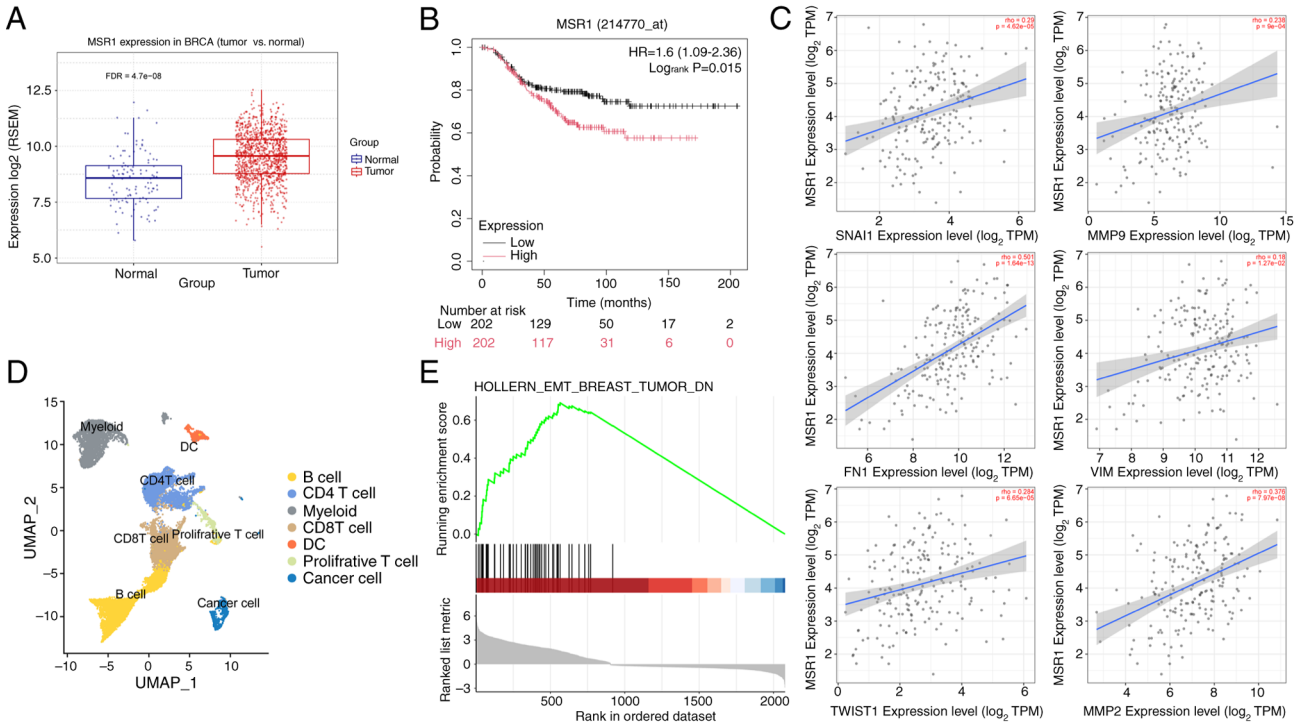

Figure 2. Tumor-associated macrophages enhance tumor metastasis in TNBC. (A) Boxplots demonstrating the differential expression of MSR1 between BRCA tumor tissue and normal tissue. (B) Overall survival analysis of MSR1 levels in TNBC. (C) Correlation analysis of MSR1 levels with Vim, Mmp-9, Snai1, Twist1, Fn1 and Mmp2 levels in TNBC. (D) UMAP analysis of total cells in mouse breast tumors. (E) Gene set enrichment analysis of the epithelial-mesenchymal transition marker levels in breast tumor. MSR1, macrophage scavenger receptor ; RSEM, RNA-sequencing by expectation maximization; BRCA, breast cancer; TPM, transcripts per million; Mmp-9, matrix metalloproteinase-9; Vim, vimentin; Fn1, fibronectin 1; MMP2, matrix metalloproteinase-2; DC, dendritic cells; FDR, false discovery rate; TNBC, triple negative breast cancer; UMAP, uniform manifold approximation and projection.

depletion of TAMs significantly reduced phosphorylated (p)-AKT expression (Fig. 4C). To assess the specific role of PI3K/AKT signaling in TAM-mediated ERβ suppression, 4T1 cells were treated with the PI3K inhibitor, LY294002, in a TAM-CM. RT-qPCR analysis revealed that PI3K/AKT pathway inhibition reversed the TAM-induced suppression of ESR2 in a dose-dependent manner (P<0.01; Fig. 4D). These findings suggested that TAM-mediated PI3K/AKT activation inhibited ESR2 transcription. Immunofluorescence assay results further corroborated these findings, showing that p-AKT and ERβ co-localize in 4T1 cells, appearing yellow in merged images, with ERβ levels increased in CM-treated 4T1 cells following PI3K/AKT inhibition, supporting an association between PI3K/AKT activation and ERβ expression (Fig. 4E).

In a previous study, whole-transcriptome profiling of 4T1 cells co-cultured with vehicle or M2 macrophages in Transwell systems revealed marked enrichment of the FOXO signaling pathway (17).

FOXO transcription factors govern diverse biological programs. Activation of the PI3K/AKT pathway results in FOXO phosphorylation, thereby influencing their localization and transcriptional regulation (30). Moreover, FOXO3a has been shown to directly drive ESR1 transcription in breast cancer (31). Therefore, it was hypothesized that TAMs suppress ERβ expression through the PI3K/AKT pathway by modulating the activity of the FOXO3a transcription factor. JASPAR (https://jaspar.elixir.no) was used to analyze the FOXO3a binding motif (Fig. 4F). The sequence 'CCTGTTTCCA' was predicted as a potential FOXO3a binding site within the mouse ESR2 promoter. ChIP assays were performed to assess FOXO3a binding to the ESR2 promoter and to determine whether activation of the PI3K/AKT pathway reduced this binding, thereby suppressing ESR2 transcription. ChIP-PCR analysis demonstrated that ESR2 was enriched by the anti-FOXO3a antibody, supporting a potential role for FOXO3a as a transcriptional regulator of ESR2 (Fig. 4G). Compared with the control group, CM treatment markedly reduced FOXO3a binding to the ESR2 promoter, whereas LY294002 treatment restored and perhaps enhanced this binding (P<0.001, Fig. 4G and H). These findings established the PI3K/AKT/FOXO3a axis as an important mechanism by which TAMs suppress ERβ expression in TNBC.

PI3K/AKT inhibition and ERβ activation inhibit tumor metastasis. Considering the invasive and migratory properties of TNBC, the effects of PI3K/AKT inhibition and ERβ activation on these properties were evaluated. Transwell assay and wound healing assays demonstrated that LY294002 treatment suppressed 4T1 cell migration. This effect was amplified when combined with the ERβ agonist, ERB041 and involved LY294002-induced ERβ upregulation (P<0.01, Fig. 5A-C). Furthermore, 4T1 cells were orthotopically implanted into the mammary fat pads of BALB/c mice, followed by their treatment with DMSO, LY294002 and LY294002 + ERB041. Metastatic lesions in the lungs were quantified and representative images of the tumor nodules in each group taken. Notably, LY294002 potently suppressed lung metastasis compared with that in

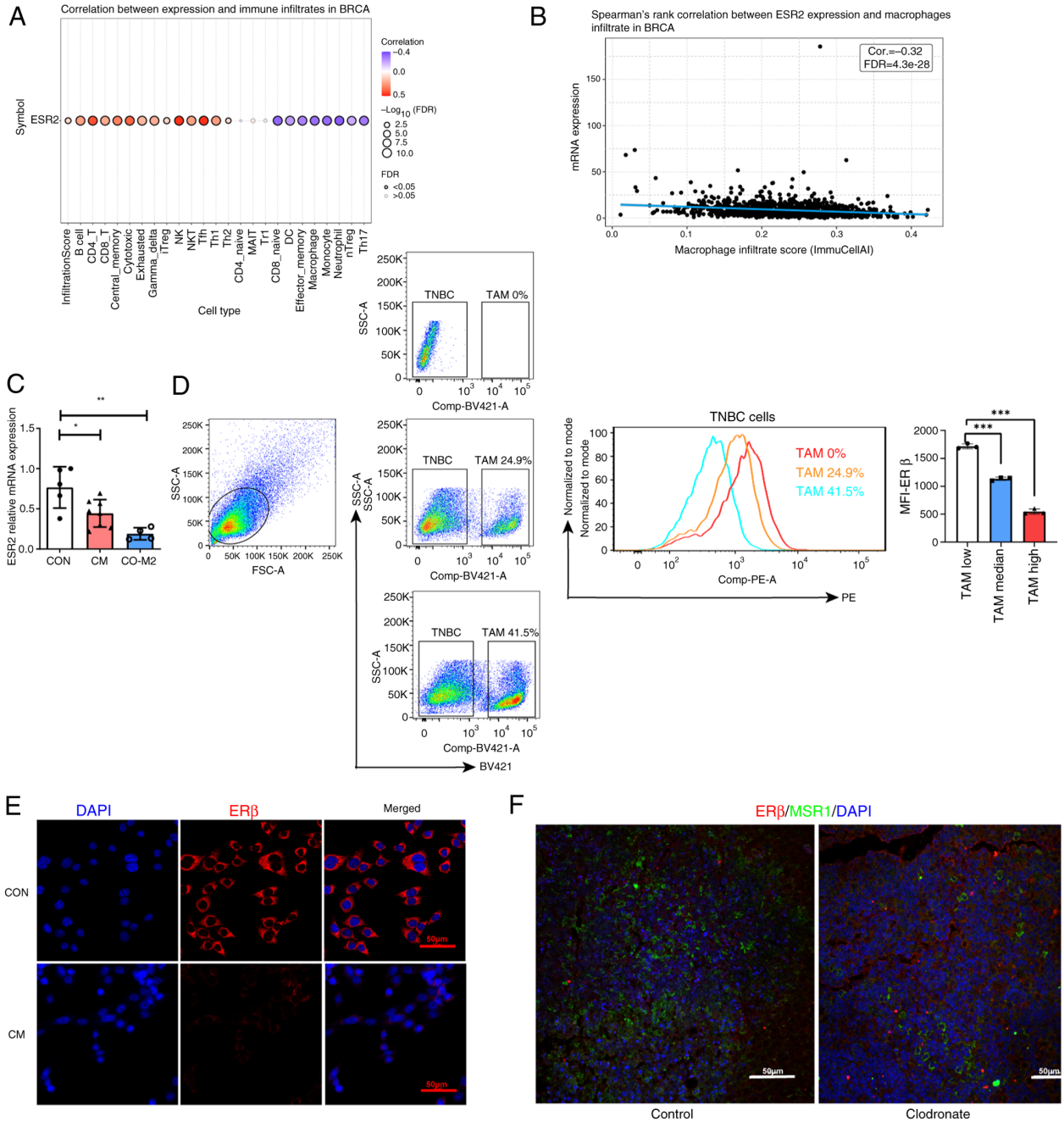

Figure 3. TAMs suppress ERβ expression in TNBC. (A) Bubble plot demonstrating the correlation between ESR2 mRNA levels and 24 immune cell type infiltrates in BRCA. Bubble size correlates with FDR. Black outline border indicates FDR ≤0.05. (B) Correlation between macrophages infiltration and ESR2 expression. (C) Relative mRNA levels of ESR2 in different groups. (D) Representative flow cytometric analysis of ERβ expression levels in 4T1 cells co-cultured with different proportion of TAMs (low, median and high) for 24 h. Mean fluorescence intensity of ERβ in the 4T1 cells of each group shown on the right (n=3). (E) Representative cellular immunofluorescence images of ERβ (red) and nuclei stained with DAPI (blue). (F) Immunofluorescence staining for MSR1 (green) and ERβ (red) in the tumor tissues of the control (left) and clodronate liposome-treated (right) groups. Original magnification, x200. Scale bars, 50 μm. *P<0.05, **P<0.01 and ***P<0.001. Comp-BV421-A represents F4/80 staining, and Comp-PE-A represents ERβ staining. ns, no significant; ERβ, estrogen receptor-β; TNBC, triple-negative breast cancer; BRCA, breast cancer; FDR, false discovery rate; TAM, tumor-associated macrophage; Cor., correlation; CON, control; CM, conditioned medium; SSC-A, side scatter-area; FSC-A, forward scatter-area; MFI, mean fluorescence intensity.

the control group. Moreover, LY294002 + ERB041 further decreased the metastatic burden (P<0.05, Fig. 5D and E). It was also observed that LY294002 significantly suppressed tumor growth (P<0.01, Figs. 5F and S1). Consistent with the *in vitro* results, PI3K/AKT activation was diminished, however ERβ expression was restored in the primary tumor of the LY294002-treated group (Fig. 5G). Body weights remained stable across all groups during treatment (Fig. S2), demonstrating no evident systemic toxicity. The present data indicated that PI3K/AKT pathway inhibition and ERβ activation suppressed metastasis in TNBC mice model.

Discussion

In the present study, findings revealed that TAMs suppressed ERβ expression in TNBC through the PI3K/AKT signaling

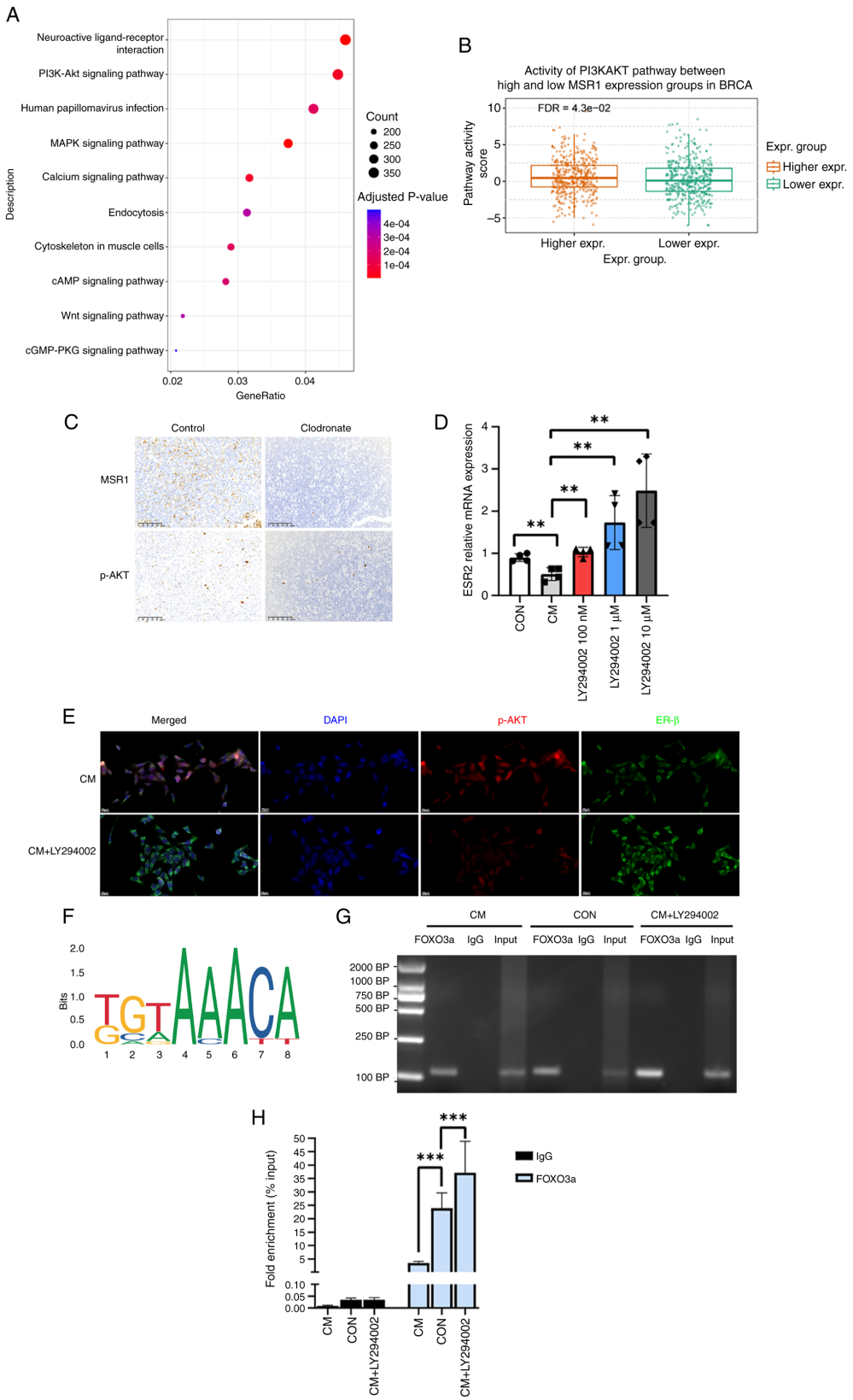

Figure 4. Tumor-associated macrophages suppress ERβ expression through the PI3K/AKT pathway. (A) Top 10 Kyoto Encyclopedia of Genes and Genomes enrichment pathways. (B) PI3K/AKT pathway activity in high and low breast cancer MSR1 expression groups. (C) Immunohistochemistry for MSR1 and p-AKT levels in the control and clodronate-treated groups. Original magnification, x200, scale bars, 100 μm. (D) 4T1 cells cultured in CM then treated DMSO or 100 nM, 1 μM or 10 μM of LY294002 for 24 h. Relative mRNA levels of ESR2 in different groups (n=4). (E) Co-localization of p-AKT and ER β in 4T1 cells. Representative cellular immunofluorescence images of 4T1 cells treated with CM or CM + LY294002 (1 μM), ERβ (green), p-AKT (red) and DAPI (blue). Original magnification, x400, scale bar, 20 μm. (F) Binding motif of FOXO3a (from JASPAR). (G) ChIP-PCR shows the binding of FOXO3a on the promoter of ESR2. Agarose gel electrophoresis of ChIP-PCR products. (H) ChIP analysis for binding of FOXO3a to the ESR2 promoter in 4T1 cells upon CM, CON or CM + LY294002 treatment for 24 h. Data are expressed as enrichment relative to the input. **P<0.01 and ***P<0.001; ns, no significant; CM, conditioned medium; ChiP; chromatin immunoprecipitation; Erβ, estrogen receptor-β; CON, control; p-AKT; phosphorylated AKT; MSR1, macrophage scavenger receptor 1; Expr., expression; FDR, false discovery rate.

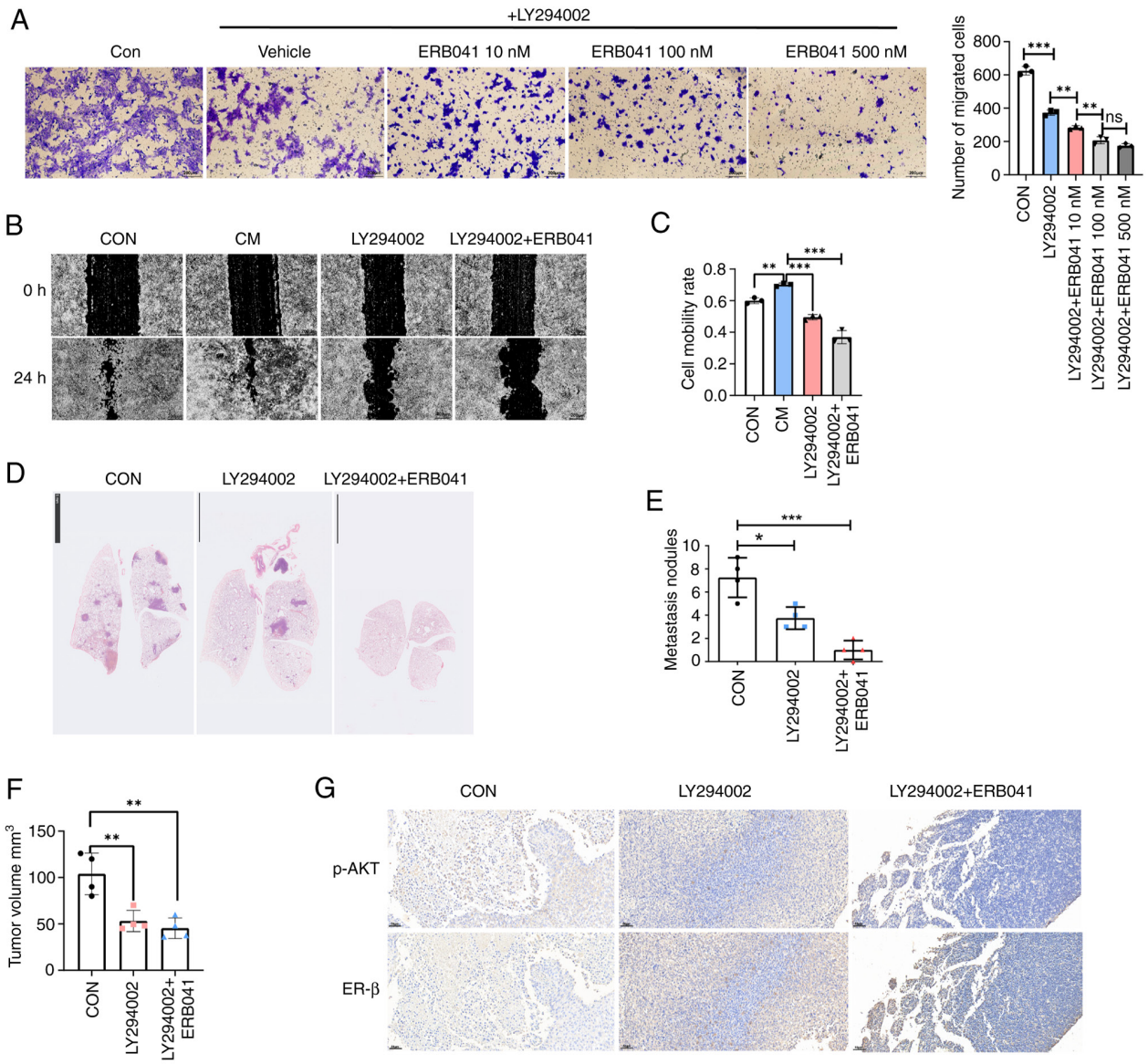

Figure 5. PI3K/AKT inhibition and ERβ activation inhibit tumor metastasis. (A) Representative images of Transwell migration assays after treatment with LY294002 (1 μM) or a combination of LY294002 and ERB041 (10-500 nM). Graph of Transwell assays (n=3). (B) Representative images of wound healing assay at 0 and 24 h after treatment with CM, LY294002 (1 μM) or a combination of LY294002 and ERB041 (100 nM). (C) Graph of wound healing assay (n=3). (D) 4T1 cells (1x10^6) were injected into the fat pads of BALB/c mice, then treated with DMSO, LY294002 (50 mg/kg intraperitoneally twice a week for five weeks) or LY294002 combined with ERB041 (5 mg/kg subcutaneously daily for five weeks). Representative images showing the H&E staining of lung metastatic nodules in 4T1 mice model. Scale bar, 5 mm (E) Lung metastatic nodule counts in different groups (n=4). (F) The volume of the 4T1 tumor across all groups (n=4). (G) Representative immunohistochemical staining images of p-AKT and ERβ in the breast tumors of different treatment groups. Scale bar, 50 μm. Magnification, x200. *P<0.05, **P<0.01 and ***P<0.001; ns, not significant. Erβ, estrogen receptor-β; CM, conditioned medium; p-AKT, phosphorylated AKT; Con, control.

pathway, thereby promoting tumor progression and metastasis. This finding highlights the key role of the tumor microenvironment in modulating therapeutic targets, outlining a potential approach to enhance ERβ-based treatment efficacy for TNBC.

TNBC is challenging to treat owing to its lack of effective therapeutic targets and aggressive and metastatic nature (32). Although ERβ exerts anti-tumor effects against TNBC (9,11,33-35), its clinical efficacy is limited due to reduced expression in tumor tissues (36). ERβ expression is gradually reduced during mammary tumorigenesis (4). Consistent with a previous report (37), the present study observed significantly downregulated ERβ levels in TNBC tumors. Therefore, the findings suggested that ERβ downregulation compromises the efficacy of ERβ agonists, marking a key event in TNBC progression. Elucidation of the mechanisms underlying such key events will facilitate the development of novel TNBC treatment strategies.

The present study focused on TAMs, the most abundant infiltrating immune cells promoting metastasis through multiple mechanisms in breast cancer (38,39). Findings revealed that the proportion of TAMs, marked by MSR1 expression, were significantly higher in TNBC tumors compared with in adjacent tissues and associated with poor overall survival. GSEA analysis revealed strong associations between TAM proportions and metastasis-related phenotypes in TNBC. Importantly, a negative correlation between

TAM infiltration and ERβ expression in breast cancer tissues was identified and subsequently validated using co-culture experiments and TAM-CM. Furthermore, in a murine model, depletion of macrophages by clodronate liposomes restored the ERβ expression in tumor tissues, further demonstrating the role of TAMs as key mediators of ERβ suppression in TNBC.

To elucidate the underlying signaling mechanisms, analysis of the pathways influenced by TAMs in TNBC samples was conducted and the significant enrichment of the PI3K/AKT pathway was observed. The PI3K/AKT pathway is a well-established oncogenic driver of TNBC (40). Consistent with a previous report of a negative correlation between PI3K/AKT activation and ERβ expression in TNBC (8), RT-qPCR analyses revealed that pharmacological blockade of the PI3K/AKT pathway reversed TAM-induced ERβ downregulation in the present study. These results suggest that TAMs suppress ERβ transcription through the PI3K/AKT pathway.

Previous work revealed marked enrichment of the FOXO signaling pathway in 4T1 cells co-cultured with M2 macrophages (17). The PI3K/AKT pathway is known to phosphorylate FOXO transcription factors, thereby altering their subcellular localization and transcriptional activity (30,31). Based on these findings, it was hypothesized that TAMs suppress ERβ expression through PI3K/AKT-mediated modulation of FOXO3a transcriptional activity. ChIP-PCR analysis identified ESR2 as a direct transcriptional target of FOXO3a. Notably, CM treatment markedly reduced FOXO3a occupancy at the ESR2 promoter, whereas PI3K/AKT blockade restored and even enhanced this binding, supporting a model in which TAM-driven PI3K/AKT activation suppresses ERβ transcription through FOXO3a.

Considering its strong anti-breast cancer activity, a number of ERβ agonists have been evaluated in clinical trials for TNBC treatment (41). However, they have demonstrated limited efficacy and ERβ expression serves as a key determinant of their efficacy in clinical trials (36).

Previous clinical trials suggest that PI3K/AKT inhibitors improve the progression-free survival of patients with metastatic TNBC (42,43). The findings of the present study revealed that blocking the PI3K/AKT pathway induced ERβ expression, warranting further investigation of the roles of ERβ-specific agonist and PI3K/AKT inhibitor combinations. In the present study, LY294002 suppressed TNBC cell migration and this effect was further magnified by the ERβ-selective agonist, ERB041. *In vitro* findings were further validated using a metastatic model, in which the combination of LY294002 and ligand-induced ERβ activation suppressed TNBC lung metastasis more potently compared with either agent alone.

In conclusion, the present study demonstrated that TAMs promoted tumor metastasis by suppressing ERβ expression through the PI3K/AKT pathway. Overall, these findings provide a mechanistic basis for the evaluation of PI3K/AKT inhibitor and ERβ-selective agonist combinations as novel therapeutic agents for TNBC.

Acknowledgements

The authors appreciate the assistance of Dr Guan Tan (Huazhong University of Science and Technology) in conducting the bioinformatics analysis.

Funding

The present study was supported by the Natural Science Foundation of Hubei Province (grant no. 2022CFB772).

Availability of data and materials

The data generated in the present study may be requested from the corresponding author.

Authors' contributions

QZ designed the study and drafted the manuscript. DG, GX and RX performed the experiments and acquired the data. QZ and DG confirm the authenticity of all the raw data. YD analyzed the data. JW and PF contributed to the conception and design of the study, and provided revisions of the manuscript. All authors read and approved the final version of the manuscript.

Ethics approval and consent to participate

All animal experiments were reviewed and approved by the Institutional Animal Care and Use Committee of Huazhong University of Science and Technology and all procedures were conducted in accordance with the institutional guidelines for the care and use of laboratory animals. Breast cancer tissues from two patients with TNBC were collected at The Central Hospital of Wuhan, Tongji Medical College, Huazhong University of Science and Technology between January 2022 and December 2023. The present study was approved by the Ethics Committee of The Central Hospital of Wuhan (approval no. WHZXKYL2022-033). Written informed consent was obtained from all patients, who also agreed to donate their surgical specimens to the Biobank of The Central Hospital of Wuhan for future breast cancer-related research.

Patient consent for publication

Not applicable.

Competing interests

The authors declare that they have no competing interests.

References

1. Siegel RL, Giaquinto AN and Jemal A: Cancer statistics, 2024. CA Cancer J Clin 74: 12-49, 2024.
2. von Minckwitz G, Untch M, Blohmer JU, Costa SD, Eidtmann H, Fasching PA, Gerber B, Eiermann W, Hilfrich J, Huober J, *et al*: Definition and impact of pathologic complete response on prognosis after neoadjuvant chemotherapy in various intrinsic breast cancer subtypes. J Clin Oncol 30: 1796-1804, 2012.
3. Hieken TJ, Carter JM, Hawse JR, Hoskin TL, Bois M, Frost M, Hartmann LC, Radisky DC, Visscher DW and Degnim AC: ERβ expression and breast cancer risk prediction for women with atypias. Cancer Prev Res (Phila) 8: 1084-1092, 2015.
4. Roger P, Sahla ME, Mäkelä S, Gustafsson JA, Baldet P and Rochefort H: Decreased expression of estrogen receptor beta protein in proliferative preinvasive mammary tumors. Cancer Res 61: 2537-2541, 2001.
5. Shaw JA, Udokang K, Mosquera JM, Chauhan H, Jones JL and Walker RA: Oestrogen receptors alpha and beta differ in normal human breast and breast carcinomas. J Pathol 198: 450-457, 2002.

6. Huang B, Omoto Y, Iwase H, Yamashita H, Toyama T, Coombes RC, Filipovic A, Warner M and Gustafsson JÅ: Differential expression of estrogen receptor α, β1, and β2 in lobular and ductal breast cancer. Proc Natl Acad Sci USA 111: 1933-1938, 2014.
7. Reese JM, Suman VJ, Subramaniam M, Wu X, Negron V, Gingery A, Pitel KS, Shah SS, Cunliffe HE, McCullough AE, *et al*: ERβ1: Characterization, prognosis, and evaluation of treatment strategies in ERα-positive and -negative breast cancer. BMC Cancer 14: 749, 2014.
8. Wang J, Zhang C, Chen K, Tang H, Tang J, Song C and Xie X: ERβ1 inversely correlates with PTEN/PI3K/AKT pathway and predicts a favorable prognosis in triple-negative breast cancer. Breast Cancer Res Treat 152: 255-269, 2015.
9. Dey P, Wang A, Ziegler Y, Kumar S, Yan S, Kim SH, Katzenellenbogen JA and Katzenellenbogen BS: Estrogen receptor beta 1: A potential therapeutic target for female triple negative breast cancer. Endocrinology 163: bqac172, 2022.
10. Zhao L, Huang S, Mei S, Yang Z, Xu L, Zhou N, Yang Q, Shen Q, Wang W, Le X, *et al*: Pharmacological activation of estrogen receptor beta augments innate immunity to suppress cancer metastasis. Proc Natl Acad Sci USA 115: E3673-E3681, 2018.
11. Reese JM, Bruinsma ES, Nelson AW, Chernukhin I, Carroll JS, Li Y, Subramaniam M, Suman VJ, Negron V, Monroe DG, *et al*: ERβ-mediated induction of cystatins results in suppression of TGFβ signaling and inhibition of triple-negative breast cancer metastasis. Proc Natl Acad Sci USA 115: E9580-E9589, 2018.
12. Mehraj U, Qayoom H and Mir MA: Prognostic significance and targeting tumor-associated macrophages in cancer: New insights and future perspectives. Breast Cancer 28: 539-555, 2021.
13. Williams CB, Yeh ES and Soloff AC: Tumor-associated macrophages: Unwitting accomplices in breast cancer malignancy. NPJ Breast Cancer 2: 15025, 2016.
14. Miyasato Y, Shiota T, Ohnishi K, Pan C, Yano H, Horlad H, Yamamoto Y, Yamamoto-Ibusuki M, Iwase H, Takeya M and Komohara Y: High density of CD204-positive macrophages predicts worse clinical prognosis in patients with breast cancer. Cancer Sci 108: 1693-1700, 2017.
15. Ning C, Xie B, Zhang L, Li C, Shan W, Yang B, Luo X, Gu C, He Q, Jin H, *et al*: Infiltrating macrophages induce ERα expression through an IL17A-mediated epigenetic mechanism to sensitize endometrial cancer cells to estrogen. Cancer Res 76: 1354-1366, 2016.
16. Stossi F, Madak-Erdoğan Z and Katzenellenbogen BS: Macrophage-elicited loss of estrogen receptor-α in breast cancer cells via involvement of MAPK and c-Jun at the ESR1 genomic locus. Oncogene 31: 1825-1834, 2012.
17. Zhang Q, Le K, Xu M, Zhou J, Xiao Y, Yang W, Jiang Y, Xi Z and Huang T: Combined MEK inhibition and tumor-associated macrophages depletion suppresses tumor growth in a triple-negative breast cancer mouse model. Int Immunopharmacol 76: 105864, 2019.
18. Chung H, Gyu-Mi P, Na YR, Lee YS, Choi H and Seok SH: Comprehensive characterization of early-programmed tumor microenvironment by tumor-associated macrophages reveals galectin-1 as an immune modulatory target in breast cancer. Theranostics 14: 843-860, 2024.
19. Livak KJ and Schmittgen TD: Analysis of relative gene expression data using real-time quantitative PCR and the 2(-Delta Delta C(T)) method. Methods 25: 402-408, 2001.
20. Jiang H, Fan D, Zhou G, Li X and Deng H: Phosphatidylinositol 3-kinase inhibitor(LY294002) induces apoptosis of human nasopharyngeal carcinoma in vitro and in vivo. J Exp Clin Cancer Res 29: 34, 2010.
21. Fujiwara M, Izuishi K, Sano T, Hossain MA, Kimura S, Masaki T and Suzuki Y: Modulating effect of the PI3-kinase inhibitor LY294002 on cisplatin in human pancreatic cancer cells. J Exp Clin Cancer Res 27: 76, 2008.
22. Guo D, Liu X, Zeng C, Cheng L, Song G, Hou X, Zhu L and Zou K: Estrogen receptor β activation ameliorates DSS-induced chronic colitis by inhibiting inflammation and promoting Treg differentiation. Int Immunopharmacol 77: 105971, 2019.
23. Chandrashekar DS, Karthikeyan SK, Korla PK, Patel H, Shovon AR, Athar M, Netto GJ, Qin ZS, Kumar S, Manne U, *et al*: UALCAN: An update to the integrated cancer data analysis platform. Neoplasia 25: 18-27, 2022.
24. Ghandi M, Huang FW, Jané-Valbuena J, Kryukov GV, Lo CC, McDonald ER III, Barretina J, Gelfand ET, Bielski CM, Li H, *et al*: Next-generation characterization of the cancer cell line encyclopedia. Nature 569: 503-508, 2019.
25. Uhlen M, Zhang C, Lee S, Sjöstedt E, Fagerberg L, Bidkhori G, Benfeitas R, Arif M, Liu Z, Edfors F, *et al*: A pathology atlas of the human cancer transcriptome. Science 357: eaan2507, 2017.
26. Li T, Fu J, Zeng Z, Cohen D, Li J, Chen Q, Li B and Liu XS: TIMER2.0 for analysis of tumor-infiltrating immune cells. Nucleic Acids Res 48 (W1): W509-W514, 2020.
27. Zhang B, Guo X, Huang L, Zhang Y, Li Z, Su D, Lin L, Zhou P, Ye H, Lu Y and Zhou Q: Tumour-associated macrophages and Schwann cells promote perineural invasion via paracrine loop in pancreatic ductal adenocarcinoma. Br J Cancer 130: 542-554, 2024.
28. Zhang L, Lu X, Xu Y, La X, Tian J, Li A, Li H, Wu C, Xi Y, Song G, *et al*: Tumor-associated macrophages confer colorectal cancer 5-fluorouracil resistance by promoting MRP1 membrane translocation via an intercellular CXCL17/CXCL22-CCR4-ATF6-GRP78 axis. Cell Death Dis 14: 582, 2023.
29. Qin Q, Ji H, Li D, Zhang H, Zhang Z and Zhang Q: Tumor-associated macrophages increase COX-2 expression promoting endocrine resistance in breast cancer via the PI3K/Akt/mTOR pathway. Neoplasma 68: 938-946, 2021.
30. Yu X, Wang R, Zhang Y, Zhou L, Wang W, Liu H and Li W: Skp2-mediated ubiquitination and mitochondrial localization of Akt drive tumor growth and chemoresistance to cisplatin. Oncogene 38: 7457-7472, 2019.
31. Jia X, Li C, Li L, Liu X, Zhou L, Zhang W, Ni S, Lu Y, Chen L, Jeong LS, *et al*: Neddylation inactivation facilitates FOXO3a nuclear export to suppress estrogen receptor transcription and improve fulvestrant sensitivity. Clin Cancer Res 25: 3658-3672, 2019.
32. Hammershoi Madsen AM, Lovendahl Eefsen RH, Nielsen D and Kumler I: Targeted treatment of metastatic triple-negative breast cancer: A systematic review. Breast J 2024: 9083055, 2024.
33. Hwang NM and Stabile LP: Estrogen receptor ß in cancer: To ß(e) or not to ß(e)? Endocrinology 162: bqab162, 2021.
34. Shanle EK, Zhao Z, Hawse J, Wisinski K, Keles S, Yuan M and Xu W: Research resource: global identification of estrogen receptor β target genes in triple negative breast cancer cells. Mol Endocrinol 27: 1762-1775, 2013.
35. Hinsche O, Girgert R, Emons G and Gründker C: Estrogen receptor β selective agonists reduce invasiveness of triple-negative breast cancer cells. Int J Oncol 46: 878-884, 2015.
36. Wisinski KB, Xu W, Tevaarwerk AJ, Saha S, Kim K, Traynor A, Dietrich L, Hegeman R, Patel D, Blank J, *et al*: Targeting estrogen receptor beta in a phase 2 study of high-dose estradiol in metastatic triple-negative breast cancer: A wisconsin oncology network study. Clin Breast Cancer 16: 256-261, 2016.
37. Gao L, Qi X, Hu K, Zhu R, Xu W, Sun S, Zhang L, Yang X, Hua B and Liu G: Estrogen receptor β promoter methylation: A potential indicator of malignant changes in breast cancer. Arch Med Sci 12: 129-136, 2016.
38. Ireland L, Santos A, Campbell F, Figueiredo C, Hammond D, Ellies LG, Weyer-Czernilofsky U, Bogenrieder T, Schmid M and Mielgo A: Blockade of insulin-like growth factors increases efficacy of paclitaxel in metastatic breast cancer. Oncogene 37: 2022-2036, 2018.
39. Fang C, Cheung MY, Chan RC, Poon IK, Lee C, To CC, Tsang JY, Li J and Tse GM: Prognostic significance of CD163+ and/or CD206+ tumor-associated macrophages is linked to their spatial distribution and tumor-infiltrating lymphocytes in breast cancer. Cancers (Basel) 16: 2147, 2024.
40. Pascual J and Turner NC: Targeting the PI3-kinase pathway in triple-negative breast cancer. Ann Oncol 30: 1051-1060, 2019.
41. Shen K, Yu H, Xie B, Meng Q, Dong C, Shen K and Zhou HB: Anticancer or carcinogenic? The role of estrogen receptor β in breast cancer progression. Pharmacol Ther 242: 108350, 2023.
42. Schmid P, Abraham J, Chan S, Wheatley D, Brunt AM, Nemsadze G, Baird RD, Park YH, Hall PS, Perren T, *et al*: Capivasertib plus paclitaxel versus placebo plus paclitaxel as first-line therapy for metastatic triple-negative breast cancer: The PAKT trial. J Clin Oncol 38: 423-433, 2020.
43. Kim SB, Dent R, Im SA, Espié M, Blau S, Tan AR, Isakoff SJ, Oliveira M, Saura C, Wongchenko MJ, *et al*: Ipatasertib plus paclitaxel versus placebo plus paclitaxel as first-line therapy for metastatic triple-negative breast cancer (LOTUS): A multicentre, randomised, double-blind, placebo-controlled, phase 2 trial. Lancet Oncol 18: 1360-1372, 2017.